

Hamburger Beiträge

zur Angewandten Mathematik

Optimally Sparse Image Approximation by Adaptive Linear Splines over Anisotropic Triangulations

Armin Iske and Laurent Demaret

Nr. 2015-05
January 2015

Optimally Sparse Image Approximation by Adaptive Linear Splines over Anisotropic Triangulations

Armin Iske

University of Hamburg
Hamburg, Germany

Email: armin.iske@uni-hamburg.de

Laurent Demaret

Helmholtz Zentrum München, ICB
Munich, Germany

Email: laurent.demaret@mail.de

Abstract—Anisotropic triangulations provide efficient methods for sparse image representations. In previous work, we have proposed a locally adaptive algorithm for sparse image approximation, *adaptive thinning*, which relies on linear splines over anisotropic Delaunay triangulations. In this contribution, we address theoretical and practical aspects concerning image approximation by linear splines over anisotropic conformal triangulations. Our discussion includes asymptotically optimal N -term approximations on relevant classes of target functions, such as horizon functions across α Hölder smooth boundaries and regular functions of $W^{\alpha,p}$ regularity, for $\alpha > 2/p - 1$. Moreover, we demonstrate the good performance of our adaptive thinning algorithm by numerical examples and comparisons.

I. INTRODUCTION

During the last few years, there has been an increasing demand in sparse representations of images, which requires constructions of suitable dictionaries $\mathcal{A} = \{\varphi_j\}_{j \in \mathbb{N}} \subset L^2([0, 1]^2)$ to obtain asymptotically optimal N -term approximations

$$\|f - f_N\|_{L^2([0,1]^2)}^2 = \mathcal{O}(N^{-\alpha}) \quad \text{for } N \rightarrow \infty, \quad (1)$$

where f_N is a linear combination of N (suitably chosen) elements from \mathcal{A} and f is assumed to lie in a function class $\mathcal{F}_\alpha \subset L^2([0, 1]^2)$ of (piecewise) regular bivariate functions, whose regularity is reflected by the parameter $\alpha > 0$.

Tensor product wavelets are well-known to provide (mildly) nonlinear approximation schemes for image approximation. In this approach, for a given wavelet orthonormal basis of $L^2([0, 1]^2)$, the N -term approximation operator W_N associates any $f \in L^2([0, 1]^2)$ with the L^2 -function $f_N = W_N f$ obtained by the N largest wavelet coefficients of f . If the chosen wavelet basis satisfies sufficient regularity and decay conditions, then the resulting decay rate of the N -term approximation (1) is related to the Besov regularity of f (see [8]).

In cases where $f \in L^2([0, 1]^2)$ is only *piecewise* smooth with singularities along (smooth) curves, N -term approximations by tensor product wavelets are of the form (cf. [9])

$$\|f - W_N f\|_{L^2([0,1]^2)}^2 = \mathcal{O}(N^{-1}) \quad \text{for } N \rightarrow \infty. \quad (2)$$

But the decay rate in (2) is only suboptimal [16]. For piecewise Hölder continuous functions f of second order with singularities along \mathcal{C}^2 -curves, decay rates of the form

$$\|f - f_N\|_{L^2([0,1]^2)}^2 = \mathcal{O}(N^{-2} (\log_2 N)^3) \quad \text{for } N \rightarrow \infty \quad (3)$$

were proven for *curvelets* by Candès and Donoho [3]. Up to the $(\log_2 N)^3$ factor, the curvelet N -term approximation rate is asymptotically optimal (see [3]). But curvelets are not adaptive to the assumed regularity of the target f . Therefore, the curvelet N -term approximation rate in (3) does not apply to functions f of less regularity, e.g., piecewise \mathcal{C}^α functions f with singularities along \mathcal{C}^α -curves, for $\alpha < 2$.

For piecewise regular images, *locally adaptive* approximation methods are of increasing interest. To this end, several concepts were developed [1], [4], [10], [11], [13], [15], [17], [18], [19], [20], [21], where the approximation schemes are essentially adapted to the (local) image geometry, rather than fixing a basis or a function frame beforehand to approximate f .

In previous work, we have developed a locally adaptive approximation method, *adaptive thinning*, which works with linear splines over anisotropic Delaunay triangulations, and which is locally adaptive to the geometric regularity of the image. As demonstrated in [5], [7], adaptive thinning leads to an efficient and competitive image compression method at computational complexity $\mathcal{O}(N \log(N))$.

In [6], we have proven asymptotically optimal N -term decay rates of the form (1) for linear spline approximation over locally adaptive anisotropic Delaunay triangulations for relevant classes of target functions f , including

- horizon functions across α Hölder smooth boundaries,
- functions of $W^{\alpha,p}$ regularity, where $\alpha > 2/p - 1$,
- piecewise regular horizon functions of $W^{\alpha,2}$ regularity.

Our constructive approach in [6] essentially depends on the local regularity of the target function f , where the resulting adaptive approximation method applies in particular to piecewise Hölder continuous horizon functions f of order $\alpha \in (1, 2]$ with singularities along α Hölder smooth boundaries.

The outline of this paper is as follows. In the following Section II, we briefly introduce linear splines over (conformal) triangulations, before we discuss nonlinear image approximation by adaptive thinning in Section III. Then, in Section IV, we explain how linear splines over locally adaptive triangulations lead to asymptotically optimal N -term approximations of the form (1) for the classes of target functions mentioned above. For the purpose of illustration we finally present in Section V numerical examples and comparisons between adaptive thinning and other relevant image approximation methods.

II. LINEAR SPLINES OVER TRIANGULATIONS

For a finite planar point set Y , a (conformal) *triangulation* $\mathcal{T} \equiv \mathcal{T}(Y)$ is a finite set $\mathcal{T} = \{T\}_{T \in \mathcal{T}}$ of triangles satisfying the following properties.

- (a) the vertex set of \mathcal{T} is Y ;
- (b) any pair of two distinct triangles in \mathcal{T} intersect at most at one common vertex or along one common edge;
- (c) the convex hull $\text{conv}(Y)$ of Y coincides with the area covered by the union of the triangles in \mathcal{T} .

A triangulation \mathcal{T} of Y is said to be a *Delaunay triangulation* of Y , iff no circumcircle of a triangle $T \in \mathcal{T}$ contains any point from Y in its interior. We recall that the Delaunay triangulation \mathcal{T} of Y is unique, provided that no four points in Y are co-circular. Moreover, there are efficient algorithms for computing the Delaunay triangulation of Y in $\mathcal{O}(N \log(N))$ steps, where $N = |Y|$ is the size of Y .

In the following of this paper, we assume that Y is a set of pixel positions, where we require that the convex hull $\text{conv}(Y)$ of Y coincides with the square image domain $[0, 1]^2$, i.e., $\text{conv}(Y) = [0, 1]^2$. Moreover, we associate with any triangulation \mathcal{T} of Y the finite dimensional linear function space of *linear splines* over \mathcal{T} ,

$$\mathcal{S}_{\mathcal{T}} := \{g \in \mathcal{C}([0, 1]^2) : g|_T \in \mathcal{P}_1 \text{ for all } T \in \mathcal{T}\},$$

containing all globally continuous functions on $[0, 1]^2$ whose restriction to any triangle $T \in \mathcal{T}$ is a linear polynomial in \mathcal{P}_1 .

Note that for any function $f \in \mathcal{C}([0, 1]^2)$, there is a unique linear spline interpolant $s \in \mathcal{S}_{\mathcal{T}}$ to f over the vertices Y of \mathcal{T} satisfying $s|_Y = f|_Y$. In particular, any linear spline $s \in \mathcal{S}_{\mathcal{T}}$ is uniquely determined by its values at the vertices Y of \mathcal{T} .

III. IMAGE APPROXIMATION BY ADAPTIVE THINNING

Adaptive thinning (AT) is a greedy pixel removal scheme, which selects a *small* subset Y of *significant pixels* from the superset of pixels in a given image. The recursive pixel removal of AT is done according to some specific removal criterion, being based on the anticipated L^2 error incurred by the removal of a vertex from a current triangulation \mathcal{T} . The selection of significant pixels Y by AT determines a (unique) Delaunay triangulation \mathcal{T} of Y , which in turn gives a spline space $\mathcal{S}_{\mathcal{T}}$. For the sake of brevity, we omit further details concerning the greedy point removal scheme AT, but rather refer to our papers [5], [7].

For the purpose of illustration, we present one numerical example, relying on the popular test image *cameraman* containing 256×256 pixels, see Figure 1 (a). In our numerical example of Figure 1, AT is used to select a set of 2,535 significant pixels from the original image, i.e., not even 3.86 % from the 65,536 given pixels. The set Y of 2,535 significant pixels are shown in Figure 1 (b) and their corresponding Delaunay triangulation $\mathcal{T}(Y)$ is in Figure 1 (c). Note that the anisotropic Delaunay triangulation $\mathcal{T}(Y)$ adapts the local geometry of the image, in particular the sharp edges therein, very well. The resulting image approximation in Figure 1 (d) is finally obtained from the evaluation of the best approximating spline from $\mathcal{S}_{\mathcal{T}(Y)}$ w.r.t. the least squares error.

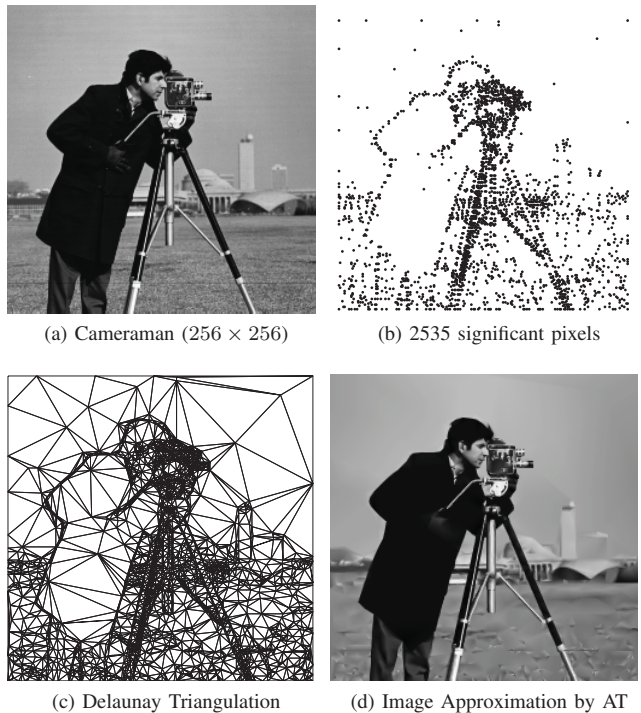


Fig. 1: Image approximation by adaptive thinning.

IV. OPTIMAL N -TERM APPROXIMATIONS

In this section, we discuss asymptotically optimal N -term approximation rates of the form (1) by linear splines over anisotropic triangulations. To this end, we explain how to construct sequences of triangulations $\{\mathcal{T}_N\}_{N \in \mathbb{N}}$, with vertex set Y_N , such that there are constants $C, M > 0$ (independent of N) satisfying the following two properties.

- (a) The size $|Y_N|$ of Y_N is bounded by $|Y_N| \leq M \times N$;
- (b) the L^2 -approximation error can be bounded above by

$$\|f - f_N\|_{L^2([0, 1]^2)} \leq CN^{-\alpha},$$

where $f_N \in \mathcal{S}(\mathcal{T}_N)$ is the unique linear interpolant to f at Y_N , and where $\alpha > 0$ is related to the regularity of f .

A. Approximation of Horizon Functions

Horizon functions [11] are popular prototypes for piecewise smooth images with discontinuities along Hölder smooth curves. To introduce the class of horizon functions, first recall that a univariate function $g : [0, 1] \rightarrow \mathbb{R}$ is said to be *Hölder continuous of order* $\beta \in (0, 1]$, $g \in \mathcal{C}^\beta([0, 1])$, iff it satisfies

$$|g(x) - g(y)| \leq C|x - y|^\beta \quad \text{for all } x, y \in [0, 1]$$

for some $C > 0$. Moreover, for $\alpha = r + \beta$, with $r \in \mathbb{N}_0$ and $\beta \in (0, 1]$, a function $g \in \mathcal{C}^r([0, 1])$ is said to be α -Hölder smooth, iff $g^{(r)} \in \mathcal{C}^\beta([0, 1])$. Finally, the linear space $\mathcal{C}^\alpha([0, 1])$ of all α -Hölder smooth functions over $[0, 1]$ is by $|g|_\alpha = \inf\{C : |g^{(r)}(x) - g^{(r)}(y)| \leq C|x - y|^\beta \forall x, y \in [0, 1]\}$ equipped with the usual semi-norm.

In the following, we only require $\alpha \in (1, 2]$, i.e., $\alpha = 1 + \beta$ for $\beta = \alpha - 1 \in (0, 1]$. In this case, $g' \in \mathcal{C}^{\alpha-1}([0, 1])$, where

$$|g'|_{\alpha-1} = |g|_{\alpha} \quad \text{for all } g \in \mathcal{C}^{\alpha}([0, 1]).$$

Now the class of α -horizon functions comprises all piecewise affine-linear functions across α -Hölder smooth horizons.

Definition 1: For any $\alpha \in (1, 2]$, a function $f : [0, 1]^2 \rightarrow \mathbb{R}$ is said to be an α -horizon function, iff it has the form

$$f(x, y) = \begin{cases} p(x, y) & \text{for } y \leq g(x), \\ q(x, y) & \text{otherwise,} \end{cases}$$

for affine-linear functions $p, q : \mathbb{R}^2 \rightarrow \mathbb{R}$ and $g \in \mathcal{C}^{\alpha}([0, 1])$ satisfying $g([0, 1]) \subset (0, 1)$. The α -Hölder smooth function $g \in \mathcal{C}^{\alpha}([0, 1])$ is called *horizon boundary* of f . \square

We can apply classical univariate spline theory to obtain a first result concerning the asymptotic decay rate for the approximation of α -horizon functions by linear splines over triangulations.

Proposition 1: For $\alpha \in (1, 2]$, let f be an α -horizon function. Then, there exist constants $C, M > 0$ (independent of N), such that for any $N \in \mathbb{N}$ there is a triangulation \mathcal{T}_N with $|\mathcal{T}_N| \leq M \times N$ vertices satisfying

$$\|f - f_N\|_{L^2([0,1]^2)}^2 \leq CN^{-\alpha}, \quad (4)$$

where $f_N \in \mathcal{S}_{\mathcal{T}_N}$ interpolates f at the vertices in \mathcal{T}_N .

Proof: Let us first remark that the asymptotic N -term approximation (4) can also be found in our previous work [6]. Nevertheless, it is quite instructive to recall the construction of \mathcal{T}_N from [6]. This is done in three steps as follows.

Step 1. We apply univariate spline interpolation to approximate the horizon boundary $g \in \mathcal{C}^{\alpha}[0, 1]$. To this end, let $S_N(g)$ be the unique linear spline interpolant to g at uniform knots, $x_i = i/N$, $i = 0, \dots, N$, of mesh width $h = 1/N$. Then, the approximation error between g and $S_N(g)$ can, over any interval $[x_i, x_{i+1}]$, be represented as

$$|g(x) - (S_N g)(x)| = \left| g(x) - g_i - \frac{g_{i+1} - g_i}{h}(x - x_i) \right|, \quad (5)$$

where we let $g_i = g(x_i)$. Since $g' \in \mathcal{C}^{\alpha-1}([0, 1])$, we have

$$\left| \frac{g_{i+1} - g_i}{h} - g'_i \right| \leq Ch^{\alpha-1} \quad \text{for some } C > 0,$$

where we let $g'_i = g'(x_i)$. But this in turn implies

$$|g(x) - (S_N g)(x)| = |g(x) - g_i - (g'_i + \mathcal{O}(h^{\alpha-1}))(x - x_i)|.$$

On the other hand, by Taylor series expansion, we have

$$g(x) = g_i + g'_i(x - x_i) + \mathcal{O}(|x - x_i|^{\alpha}),$$

so that (5) can further be rewritten as

$$|g(x) - (S_N g)(x)| = \mathcal{O}(|x - x_i|^{\alpha}) + \mathcal{O}(h^{\alpha}) = \mathcal{O}(h^{\alpha}).$$

This yields the uniform bound

$$\|g - S_N(g)\|_{L^{\infty}([0,1])} \leq Ch^{\alpha} = CN^{-\alpha}$$

for some constant $C > 0$ independent of N .

Step 2. We approximate f by functions f_N of the form

$$f_N(x, y) = \begin{cases} p(x, y) & \text{for } y \leq (S_N g)(x) - \varepsilon_N, \\ q(x, y) & \text{for } y \geq (S_N g)(x) + \varepsilon_N, \\ g_N(x, y) & \text{otherwise,} \end{cases}$$

for sufficiently small constants $\varepsilon_N > 0$ (specified in step 3), such that the functions f_N are uniformly bounded on $[0, 1]^2$,

$$\|f_N\|_{L^{\infty}([0,1]^2)} \leq \|f\|_{L^{\infty}([0,1]^2)} \quad \text{for all } N \in \mathbb{N}.$$

Note that f_N coincides with f outside the ε_N -corridor

$$K_{\varepsilon_N} = \{(x, y) \in [0, 1]^2 : |y - (S_N g)(x)| \leq \varepsilon_N\},$$

so that

$$\begin{aligned} \|f - f_N\|_{L^2([0,1]^2)}^2 &= \int_{K_{\varepsilon_N}} |f(x, y) - f_N(x, y)|^2 dx dy \\ &\leq 4\|f\|_{L^{\infty}([0,1]^2)}^2 \int_{K_{\varepsilon_N}} dx dy \\ &= 8\|f\|_{L^{\infty}([0,1]^2)}^2 \varepsilon_N. \end{aligned}$$

Step 3. Now it is rather straightforward to construct a triangulation \mathcal{T}_N , whose associated linear spline interpolant to f is a function of the form f_N . Indeed, we can triangulate the union $Y_N = \mathcal{I}_N \cup \mathcal{B}_N$ of the $2(N+1)$ interior points

$$\mathcal{I}_N = \{(x_i, (S_N g)(x_i) \pm \varepsilon_N) : i = 0, \dots, N\} \subset [0, 1]^2$$

and the $2(N+1)$ (horizontal) boundary points

$$\mathcal{B}_N = \{(x_i, 0), (x_i, 1) : i = 0, \dots, N\} \subset [0, 1]^2$$

to obtain the desired triangulation \mathcal{T}_N (see [6]), which in turn yields the unique linear spline interpolant $f_N \in \mathcal{S}_{\mathcal{T}_N}$ to f with

$$\|f - f_N\|_{L^2([0,1]^2)}^2 \leq 8\|f\|_{L^{\infty}([0,1]^2)}^2 \varepsilon_N.$$

Now we finally let $\varepsilon_N = h^{\alpha} = N^{-\alpha}$, which then yields the stated error estimate in (4) for $C = 8\|f\|_{L^{\infty}([0,1]^2)}^2$. \blacksquare

We remark that the decay rate $\mathcal{O}(N^{-\alpha/2})$ in (4) is *optimal*, i.e., no polynomial depth search dictionary can achieve better decay rates for the class of α -horizon functions. This result is proven in [14] by using arguments from estimation theory.

B. Approximation of Regular Functions

Now we turn to the approximation of *regular* functions from Sobolev spaces $W^{\alpha,p}([0, 1]^2)$, for $\alpha \in (0, 2]$ and $p \geq 1$, where we assume $\alpha > 2/p - 1$. In this case, $W^{\alpha,p}([0, 1]^2)$ is embedded in $L^2([0, 1]^2)$ (see e.g. [12, Subsection 2.5.1]), but does not lie on the $L^2([0, 1]^2)$ embedding line. For the sake of brevity, we then say that $W^{\alpha,p}([0, 1]^2)$ *lies above the L^2 -embedding line*.

We will essentially adapt our approximation scheme to the regularity of f . Note that regular functions are isotropic and, moreover, they can be characterised by the asymptotic behaviour of their wavelet coefficients. We remark that the class of regular functions form a rather large subset in the linear space of all functions which can be approximated by classical nonlinear (tensor product) wavelet approximations at a decay rate $\mathcal{O}(N^{-\alpha/2})$, for $N \rightarrow \infty$.

In the following error analysis of this section, we rely on a classical result by Birman-Solomjak [2] concerning approximation of regular functions by piecewise-affine functions over quadtree partitions of $[0, 1]^2$.

Theorem 1 (Birman-Solomjak): Let $f \in W^{\alpha,p}([0, 1]^2)$ for $\alpha \in (0, 2]$ and $p \geq 1$ satisfying $\alpha > 2/p - 1$. Then there exists a constant $C > 0$ (independent of N), such that for any $N \in \mathbb{N}$ there is a quadtree partition \mathcal{Q}_N of $[0, 1]^2$ with $|\mathcal{Q}_N| \leq N$ leaves satisfying

$$\|f - f_N\|_{L^2([0,1]^2)}^2 \leq CN^{-\alpha}, \quad (6)$$

where $f_N = \Pi_{\mathcal{Q}_N} f$ is the orthogonal L^2 -projection of f onto the space of piecewise affine-linear (but not necessarily continuous) functions over the quadtree partition \mathcal{Q}_N . \square

We remark that the proof of Birman-Solomjak is constructive. In particular, an explicit algorithmic construction of a quadtree partition \mathcal{Q}_N satisfying the error estimate (6) is provided in [2]. But \mathcal{Q}_N does not necessarily minimize the approximation error in (6) among all quadtree partitions \mathcal{Q} of size $|\mathcal{Q}| \leq N$. This may affect the size of the constant C but not the asymptotic decay rate in (6).

Now we turn to the approximation of regular functions by adaptive linear splines over anisotropic triangulations. We can construct a sequence of triangulations \mathcal{T}_N , such that the corresponding sequence of orthogonal L^2 -projections $\Pi_{\mathcal{T}_N} f$ of f onto the space $\mathcal{S}_{\mathcal{T}_N}$ of linear splines over \mathcal{T}_N achieves the same approximation rate as the sequence of functions $\Pi_{\mathcal{Q}_N} f$ from the Birman-Solomjak theorem.

Corollary 1: Suppose $f \in W^{\alpha,p}([0, 1]^2)$ for $\alpha \in (0, 2]$ and $p \geq 1$ satisfying $\alpha > 2/p - 1$. Then there exist constants $C, M > 0$ (independent of N), such that for any $N \in \mathbb{N}$ there is a triangulation \mathcal{T}_N of size $|\mathcal{T}_N| \leq M \times N$ satisfying

$$\|f - \Pi_{\mathcal{T}_N} f\|_{L^2([0,1]^2)}^2 \leq CN^{-\alpha},$$

where $\Pi_{\mathcal{T}_N} f$ is the orthogonal L^2 -projection of f onto $\mathcal{S}_{\mathcal{T}_N}$.

Proof: We split the proof into three steps.

Step 1. Let $\{\mathcal{Q}_N\}_N$ denote the sequence of quadtree partitions from the Birman-Solomjak theorem, satisfying (6). By $V_{\mathcal{Q}_N} = \{(x_m, y_m)\}_{m=1, \dots, M}$ we denote, for any $N \in \mathbb{N}$, the vertex set of \mathcal{Q}_N , comprising all M vertices from the $|\mathcal{Q}_N| \leq N$ quadtree leaves, so that $M \leq 4 \times N$.

Next we associate, for some (sufficiently small) $\varepsilon > 0$, the vertex set $V_{\mathcal{Q}_N}$ with the perturbed planar point set

$V_{M,\varepsilon} = (\{(x_m \pm \varepsilon, y_m \pm \varepsilon) : m = 1, \dots, M\} \cap [0, 1]^2) \cup V$ unioned with the vertex set $V = \{(0, 0), (0, 1), (1, 0), (1, 1)\}$.

Step 2. Now we construct a triangulation $\mathcal{T}(V_{M,\varepsilon})$ of the perturbed point set $V_{M,\varepsilon}$. To this end, we partition the domain $[0, 1]^2$ into a set of disjoint areas, M small subsquares s_m , N large subsquares S_n , and K anisotropic rectangles R_k , such that their union is $[0, 1]^2$. The small subsquares are

$s_m = \text{conv}\{(x_m \pm \varepsilon, y_m \pm \varepsilon)\} \cap [0, 1]^2$ for $m = 1, \dots, M$,

the large subsquares are, for $i, j = 0, \dots, 2^k - 1$ of the form

$$S_n = \left[\frac{i}{2^k} + \varepsilon, \frac{i+1}{2^k} - \varepsilon \right] \times \left[\frac{j}{2^k} + \varepsilon, \frac{j+1}{2^k} - \varepsilon \right]$$

for $n = 1, \dots, N$, and the anisotropic rectangles R_k are given by the complement $[0, 1]^2 \setminus \left(\left(\bigcup_{m=1}^M s_m \right) \cup \left(\bigcup_{n=1}^N S_n \right) \right)$.

To obtain a triangulation $\mathcal{T}(V_{M,\varepsilon})$ of $V_{M,\varepsilon}$, it is straightforward to triangulate the subsquares s_m and S_n and the rectangles R_k , by splitting each subdomain, s_m , S_n , or R_k , across any of its two diagonals.

Step 3. Finally, let $f_N \in \mathcal{S}_{\mathcal{T}_N}$, $\mathcal{T}_N = \mathcal{T}(V_{M,\varepsilon})$, be the unique linear spline function which interpolates the piecewise affine-linear Birman-Solomjak function $\Pi_{\mathcal{Q}_N} f$ in (6) at the vertices $V_{M,\varepsilon}$. Note that f_N coincides with $\Pi_{\mathcal{Q}_N} f$ on each large subsquare S_n , and therefore

$$\begin{aligned} \|f_N - \Pi_{\mathcal{Q}_N} f\|_{L^2([0,1]^2)}^2 &= \sum_{m=1}^M \|f_N - \Pi_{\mathcal{Q}_N} f\|_{L^2(s_m)}^2 \\ &\quad + \sum_{k=1}^K \|f_N - \Pi_{\mathcal{Q}_N} f\|_{L^2(R_k)}^2. \end{aligned}$$

Now we can bound the L^2 -error over any small square s_m by

$$\|f_N - \Pi_{\mathcal{Q}_N} f\|_{L^2(s_m)}^2 \leq C \|\Pi_{\mathcal{Q}_N} f\|_{\infty}^2 4\varepsilon^2$$

for some constant $C > 0$ independent of N . Likewise, we can bound the L^2 -error over any rectangle R_k by

$$\|f_N - \Pi_{\mathcal{Q}_N} f\|_{L^2(R_k)}^2 \leq C \|\Pi_{\mathcal{Q}_N} f\|_{\infty}^2 2\varepsilon$$

for some constant $C > 0$ independent of N . This then yields

$$\begin{aligned} \|f - \Pi_{\mathcal{T}_N} f\|_{L^2([0,1]^2)}^2 &\leq \|f - f_N\|_{L^2([0,1]^2)}^2 \\ &\leq \|f - \Pi_{\mathcal{Q}_N} f\|_{L^2([0,1]^2)}^2 + \|f_N - \Pi_{\mathcal{Q}_N} f\|_{L^2([0,1]^2)}^2 \\ &\leq CN^{-\alpha} + C\varepsilon, \end{aligned}$$

for arbitrarily small ε . We let $\varepsilon = N^{-\alpha}$ to complete our proof. \blacksquare

In conclusion, we wish to make two final remarks.

Firstly, by Corollary 1, any regular $f \in W^{\alpha,p}([0, 1]^2)$, $\alpha > 2/p - 1$, can be approximated by linear splines over triangulations at an N -term decay rate of $\mathcal{O}(N^{-\alpha/2})$. But this approximation rate is *optimal*, since it is at least as good as that of nonlinear wavelet approximation. In fact, the asymptotic decay rate $\mathcal{O}(N^{-\alpha/2})$ of wavelet representations is optimal for the Sobolev spaces $W^{\alpha,p}([0, 1]^2)$ in Corollary 1 (see [11]).

Secondly, although the proof the Birman-Solomjak theorem in [2] is constructive, it does not provide a sequence of *optimal* quadtree partitions, $\{\mathcal{Q}_N^*\}$, satisfying

$$\|f - \Pi_{\mathcal{Q}_N^*} f\|_{L^2([0,1]^2)} = \inf_{\mathcal{Q}_N} \|f - \Pi_{\mathcal{Q}_N} f\|_{L^2([0,1]^2)}.$$

As we rely on the Birman-Solomjak quadtree partitions \mathcal{Q}_N , the triangulations \mathcal{T}_N in Corollary 1 are not optimal either.

But our greedy approximation algorithm, *adaptive thinning*, achieves to construct a sequence of anisotropic Delaunay triangulations $\{\mathcal{T}_N^*\}_N$ whose corresponding spline approximations $f_N^* \in \mathcal{T}_N^*$ improve the approximation quality of the approximations $\Pi_{\mathcal{T}_N} f$ output by Corollary 1 quite significantly. This is supported by our extensive numerical results, two of which we briefly present in the following Section V.

V. NUMERICAL RESULTS

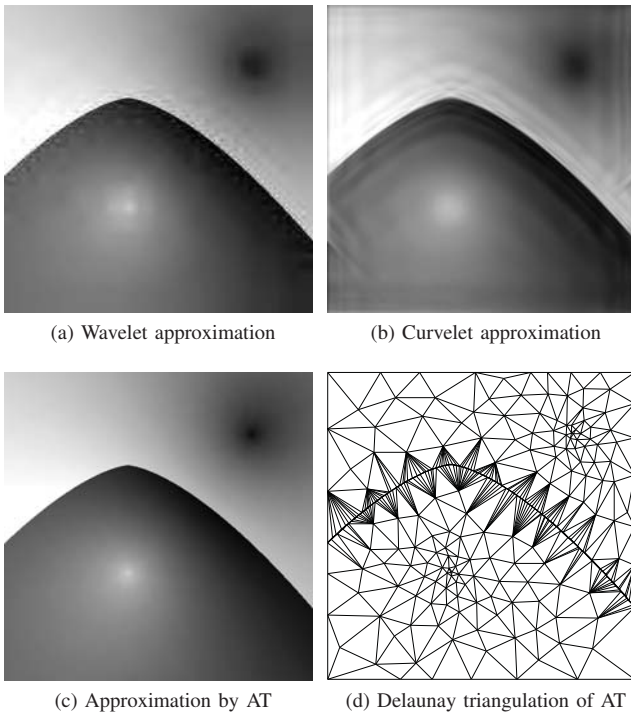


Fig. 2: Approximation to a piecewise regular function.

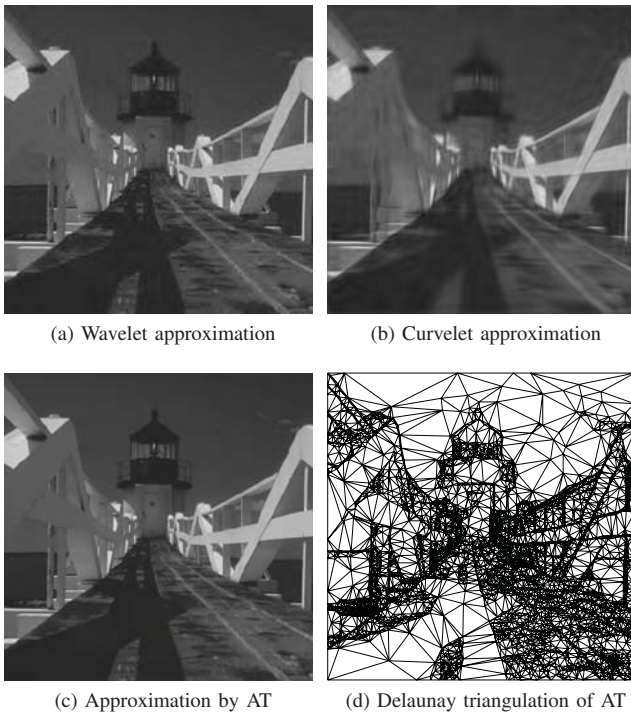


Fig. 3: Approximation to a natural image.

TABLE I: Approximation to a piecewise regular function (left columns) and to a natural image (right columns).

Method	# terms	PSNR	# terms	PSNR
Wavelets	655 coeffs	34.26 dB	6553 coeffs	33.61 dB
Curvelets	1478 coeffs	29.78 dB	14780 coeffs	30.32 dB
AT	400 vertices	50.00 dB	6000 vertices	36.58 dB

For the purpose of illustration, we consider presenting two numerical examples. Our numerical results are reflected by Table I and Figures 2,3. We can conclude that approximation by adaptive thinning (AT) is quite competitive. Given the page limits, we need to finish here. Further explanations on our numerical results could be provided during the conference.

REFERENCES

- [1] F. Arandiga, A. Cohen, R. Donat, N. Dyn, and B. Matei: Approximation of piecewise smooth functions and images by edge-adapted (ENO-EA) nonlinear multiresolution techniques. *Appl. Comput. Harmon. Anal.* **24**, 2008, 225–250.
- [2] M. Birman and M. Solomjak: Piecewise-polynomial approximations of functions of the classes W_p^s . *Math. USSR-Sbornik* **2**(3), 1967.
- [3] E. Candés, and D. Donoho: New tight frames of curvelets and optimal representations of objects with piecewise C^2 singularities. *Comm. Pure Appl. Math.* **57**(2), 2004, 219–266.
- [4] S. Dekel and D. Leviatan: Adaptive multivariate approximation using binary space partitions and geometric wavelets. *SIAM J. Numer. Anal.* **43**, 2006, 707–732.
- [5] L. Demaret, N. Dyn, and A. Iske: Image compression by linear splines over adaptive triangulations. *Signal Processing Journal* **86**(7), July 2006, 1604–1616.
- [6] L. Demaret and A. Iske: Optimal N-term approximation by linear splines over anisotropic Delaunay triangulations. *Mathematics of Computation*. Published electronically, October 17, 2014.
- [7] L. Demaret and A. Iske: Adaptive image approximation by linear splines over locally optimal Delaunay triangulations. *IEEE Signal Processing Letters* **13**(5), May 2006, 281–284.
- [8] R. DeVore: Nonlinear approximation. *Acta Numerica* **7**, 1998, 51–150.
- [9] R. DeVore, B. Jawerth, and B. Lucier: Image compression through wavelet transform coding. *IEEE Transact. Informat. Theory* **38**(2), 1992.
- [10] M.N. Do and M. Vetterli: The contourlet transform: an efficient directional multiresolution image representation. *IEEE Transactions on Image Processing* **14**(12), December 2005, 2091–2106.
- [11] D. Donoho: Wedgelets: nearly-minimax estimation of edges. *Ann. Stat.* **27**, 1999, 859–897.
- [12] D.E. Edmunds and H. Triebel: *Function Spaces, Entropy Numbers and Differential Operators*. Cambridge University Press, 1996.
- [13] L. Jaques and J.-P. Antoine: Multiselective pyramidal decomposition of images: wavelets with adaptive angular selectivity. *Int. J. Wavelets Multiresolut. Inf. Process.* **5**, 2007, 785–814.
- [14] A. Korostelev and A. Tsybakov: *Minimax Theory of Image Reconstruction*, Springer, 1993.
- [15] E. Le Pennec and S. Mallat: Banded image approximation and compression. *Multiscale Model. Simul.* **4**, 2005, 992–1039.
- [16] S. Mallat: *A Wavelet Tour of Signal Processing*. Academic Press, 1999.
- [17] S. Mallat: Geometrical grouplets. *Appl. Comput. Harmon. Anal.* **26**, 2009, 161–180.
- [18] G. Plonka: The easy path wavelet transform: a new adaptive wavelet transform for sparse representation of two-dimensional data. *Multiscale Modelling Simul.* **7**, 2009, 1474–1496.
- [19] D.D. Po and M.N. Do: Directional multiscale modeling of images using the contourlet transform. *IEEE Trans. Image Proc.* **15**, 2006, 1610–1620.
- [20] R. Shukla, P.L. Dragotti, M.N. Do, and M. Vetterli: Rate-distortion optimized tree structured compression algorithms for piecewise smooth images. *IEEE Trans. Image Process.* **14**, 2005, 343–359.
- [21] M.B. Wakin, J.K. Romberg, H. Choi, and R.G. Baraniuk: Wavelet-domain approximation and compression of piecewise smooth images. *IEEE Trans. Image Process.* **15**, 2006, 1071–108.